

## Visualization of the Plasma Processes at Additional Lower Hybrid Heating on the FT-2 Tokamak

S.I. Lashkul, A.B. Altukhov, A.O. Bogdanenko\*, E.O. Vekshina\*, V.V. Dyachenko,  
L.A. Esipov, S.V. Shatalin\*

A.F.Ioffe Physico-Technical Institute, Politekhnikeskaya 26, 194021, St.Petersburg, Russia,  
[Serguey.Lashkul@mail.ioffe.ru](mailto:Serguey.Lashkul@mail.ioffe.ru)

\*St.Petersburg State Polytechnical University, St.Petersburg, Russia

(I) A video camera allows us fairly well to obtain more detailed and demonstrable information from plasma experiments on tokamaks. In the Lower Hybrid Heating (LHH) experiment [1] at the FT-2 tokamak, where a black and white upgraded television video camera (VC) was used as a receiver of the monochromatic light of a grating spectrometer, the characteristic features of the hydrogen recycling near a plasma periphery have been obtained [2]. The neutral hydrogen recycling decreases during LHH followed by the L-H transition, leading to a change of the atom/molecular mixture near the limiter. The method of finding the atomic hydrogen H and molecular hydrogen H<sub>2</sub> density is based on comparison of observed Balmer lines intensities of atomic hydrogen [3]. The LHH experiment shows that the intensity

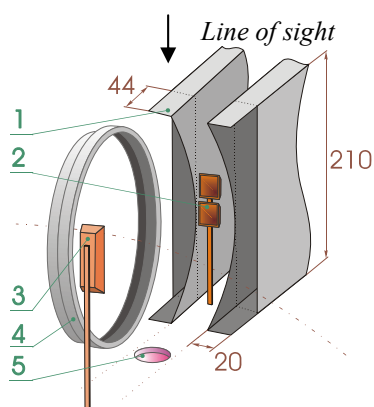


Fig.1 Interior of the chamber section with two waveguide LH grill

ratio of hydrogen emission lines  $H_{\beta}/H_{\alpha}$  at the periphery changes from  $0.2 \div 0.22$  to  $0.30 \div 0.32$  during LHH and L - H transition [2]. This trend indicates an arbitrary decrease of hydrogen molecular content (from  $H_2/H \sim 10$  to  $\sim 0$ ) at L - H transition, which seems to be a result of reduction of the direct interaction of the plasma column with the limiter and chamber wall, which are sources of cold molecular H<sub>2</sub> fluxes [2]. On the other hand, rise of the  $H_{\beta}/H_{\alpha}$  intensities ratio (in correspondence with [4, 5])

reveals the fact that principal quantum numbers  $n > 2$  of hydrogen atoms are probably mainly populated via recombination [4]. So, by analogy with [5], one can suggest that the plasma column detaches from the limiter.

This paper deals with new LHH experiments (which are similar to one presented in [2, 6]), where an upgraded television camera has been used for visualization of the plasma processes

near the limiter and the two-waveguide grills. Fig. 1 depicts the section of the chamber interior with a two-waveguide LH grill,

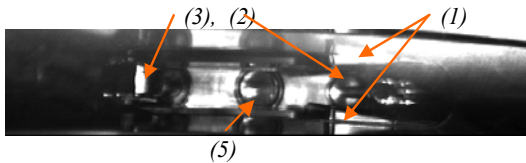


Fig.2 The view through top diagnostic port: (1) - two waveguide LH grill antenna. (2, 3) - horns of microwave diagnostics. (5) - diagnostic hole.

by the arrow. Fig. 2 shows chamber interior attributes (view from the top diagnostic port).

The upgraded video camera enables to grab the plasma images with video outputs of 20ms as

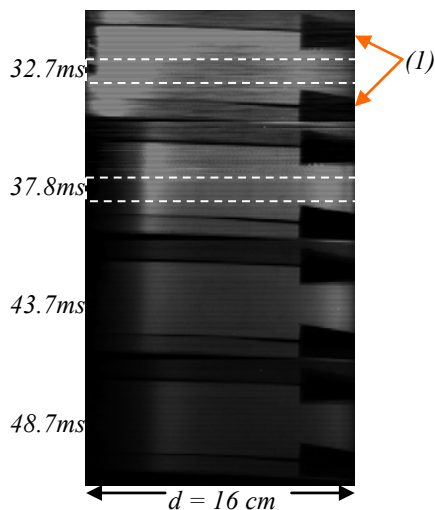


Fig.3 The sequence of the exposed plasma column images. Dashed lines selects the parts of the plasma column considered for profile intense graphics (see fig. 4).

well as 10ms, 5ms and 2.5ms per half-frame. An example of the sequence of images of the plasma column grabbed with video output of 5ms per half-frame is presented in Fig 3 for LHH experiment with  $P_{LHH} \approx 160\text{kW}$ ,  $\Delta t_{LH} = 9\text{ms}$ ,  $f = 920\text{MHz}$  (typical with [6]). Integration time was 1ms. The spectral interval covered by VC is within 450nm – 750nm range. Fig. 4 depicts chord radiation intensity profiles of the selected plasma column image, which are marked with dotted lines on Fig. 3. The space resolution of the used layout of the VC was  $\sim 0.2\text{mm}$ . The minor diameter of the poloidal limiter is  $d = 16\text{cm}$ . The time history of the main experimental data  $I_{pl}$ ,  $U_p$ , as well as central  $T_i(t, r=0\text{cm})$  and  $\langle n_e(t) \rangle$  are presented

in Fig. 5. This figure also demonstrates a decrease in the  $H_\beta$  line intensity at L – H transition, the controlled outward column shift ( $\Delta U_r$  – signal) as well as displays marked moments of the video images (red boxes).

One may notice from Fig. 3 and 4 a shift of plasma column outward along the major radius R as well as a decrease of the minor column diameter and significant decrease of the radiation, which is a

result of an abrupt decrease of the plasma - wall (limiter) interaction. Observed processes are

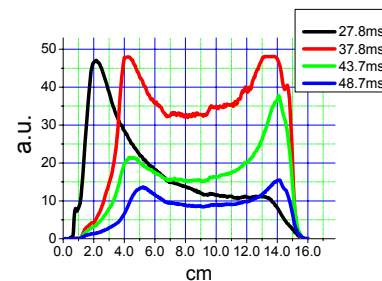


Fig. 4 Chord profiles of the plasma radiation for selected part (Fig. 3) of the plasma column.

in agreement with a decrease of plasma radiation losses at the plasma periphery, sharpening

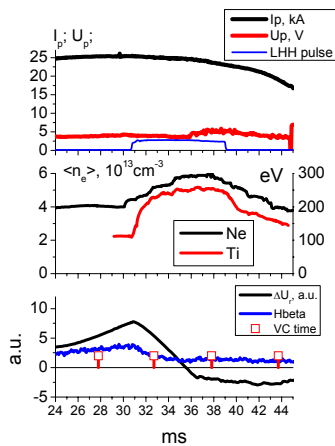


Fig. 5 The time history of the main experimental data. Moments of the video images are marked by red boxes.

of the plasma current density  $j(\rho)$  and an abrupt decrease in the density and temperature in the SOL measured by Langmuir probes [6] as well as a change of the atom/molecular ratio in the neutral hydrogen gas composition at the plasma periphery (mentioned above). The obtained video images of the plasma column permitted to prove the conclusions based on the spectroscopic data and data from other diagnostics, stating that the dense high temperature plasma column is slightly shifted outward along of the major radius (see change of  $\Delta U_r$  in Fig. 5) at additional LHH with a reduction of the column diameter. The reduction  $\Delta d$  could be estimated as 1.5 - 2cm (see Fig. 4).

(II) Observations of the dust formations in the plasma region (where the two-waveguide grill is located) have been done for the first time with a video camera. Dust generation is caused by

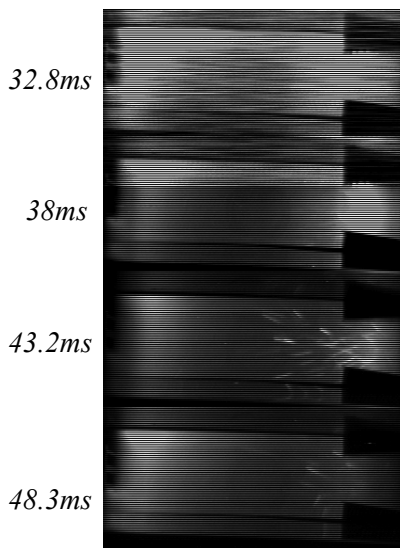


Fig. 6 Dust generation caused by micro breakdowns between the waveguides

micro breakdowns between the waveguides of the grill, which sometimes are observed as shown in Fig. 6 for 38ms ( $\Delta t_{LH}$  is from 31ms to 40ms). One can see dust particles appear at the end of the LHH pulse (38ms), the traces of the particles can be seen for 15ms. Dust particles might be a main source of plasma impurities in the hot plasma of fusion devices. One guesses that the main suppliers of the dust particles are the divertor plates with the highest energy loads [7, 8]. However, video observation in the LHH experiment on the FT-2 tokamak indicates that the waveguides of the grill on tokamaks can be a source of the dust and cluster particles also. Erosion processes and co-deposition results in the formation of mixed material layers whose chemical and thermo-mechanical properties differ from the original wall materials [7]. Thick co-deposits may peel off thus leading to the dust formation. In our case the thin deposit was observed on the segment of the diagnostic antenna (marked with (2) on Fig. 1). The flaking metal/carbon deposits covered the horn of the antenna after a long exposure to the plasma at the FT-2 tokamak. The first

observations by VC demonstrate various characters of the dust particles movements from the plasma periphery inward to the plasma column. Tracks of dust recorded at the video images allowed us to estimate the “flight” velocity of dust particles, which varies from a fraction of a meter per second to a few tens of meters per second. The main forces acting on a dust particle are considered to be the following ones: the electric force, the gravity force, the



*Fig. 7 The example of the debris motion, it seems caused by the rocket effect.*

magnetic force, the reactive force, as well as the plasma–dust particle friction force [8]. The example of the debris motion caused by the rocket effect is presented in Fig. 7. The rocket effect in the particle motion is related to the difference in heat fluxes from the ion and electron drift sides [7]. The electric and friction forces are the main forces that influence the migration of the dust particles.

Interactions of dust particles with surface chamber inhomogeneities can also cause an

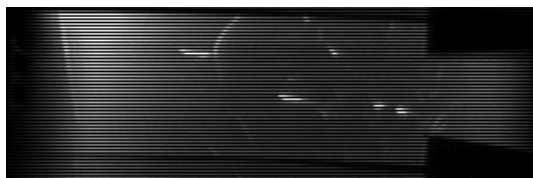


*Fig. 8 The example of the complex dust trajectory*

escape of dust particles from the near wall region and flight towards the tokamak core [8]. An example of the complex dust trajectory, which could be result of interaction of dust particles with some micro-roughness of the surface chamber, is presented in Fig. 8. So, the characteristic features of the dust particles generation and the mechanisms of their movement could be studied using television camera images. One of the important tasks of this work is connected with a study of high RF power launch conditions for optimization of the plasma additional heating.

*This work was supported by RFBR 08-02-00610, 07-02-00895, 06-02-16785, NWO-RFBR Grant 047.016.015, NSH-1550.2008.2, INTAS 05-1000008-8046 and “Rus. Science Support Foundation” grants.*

## References

1. S.I.Lashkul, V.N.Budnikov, et al. *Pl. Phys. and Contr Fus*, 2000, v.42 p. A169 - A174
2. S.I. Lashkul, et al. *Proc. of the 34th EPS and Pl. Phys. Warshava*, 2007, P2.148
3. Keiji Sawada, Kouji Eriguchi and Takashi Fojimoto. *J. Appl.Phys.*73(12), 15 June 1993
4. G. Sergienco et all. *Jornal of Nuclear Materials* 290 – 293 (2001) 720 – 724
5. G.M.McCracken, M.F.Stamp, R.D.Monk et al., *Nucl. Fus*, Vol.38, No. 4 (1998) 619
6. S.I. Lashkul et al. *Proc. of the 34th EPS and Pl. Phys. Warshava*, 2007, P2.055
7. Marek Rubel. *Physica Scripta*. T123 (2006) 54–65
8. Krasheninnikov S.I. et al. *Phys. Plasmas*, Vol. 11, No. 6, June 2004